Taylor & Francis
Taylor & Francis Group

ORIGINAL RESEARCH

OPEN ACCESS | Check for updates

Piezo1 facilitates optimal T cell activation during tumor challenge

muta abiff[a], Mohammad Alshebremi[a,b], Melissa Bonner [iD][a], Jay T. Myers [iD][c], Byung-Gyu Kim [iD][c], Suzanne L. Tomchuck [iD][c], Alicia Santin [iD][a], Daniel Kingsley [iD][a], Sung Hee Choi [iD][c], and Alex Y. Huang [iD][a,c,d]

[a]Department of Pathology, Case Western Reserve University School of Medicine, Cleveland, OH, USA; [b]Department of Medical Laboratories, College of Applied Medical Sciences, Qassim University, Buraydah, Saudi Arabia; [c]Pediatrics, Case Western Reserve University School of Medicine, Cleveland, OH, USA; [d]Center for Pediatric Immunotherapy, Angie Fowler AYA Cancer Institute, UH Rainbow Babies & Children's Hospital, Cleveland, OH, USA

ABSTRACT

Functional effector T cells in the tumor microenvironment (TME) are critical for successful anti-tumor responses. T cell anti-tumor function is dependent on their ability to differentiate from a naïve state, infiltrate into the tumor site, and exert cytotoxic functions. The factors dictating whether a particular T cell can successfully undergo these processes during tumor challenge are not yet completely understood. Piezo1 is a mechanosensitive cation channel with high expression on both $CD4^+$ and $CD8^+$ T cells. Previous studies have demonstrated that Piezo1 optimizes T cell activation and restrains the $CD4^+$ regulatory T cell (T_{reg}) pool in vitro and under inflammatory conditions in vivo. However, little is known about the role Piezo1 plays on $CD4^+$ and $CD8^+$ T cells in cancer. We hypothesized that disruption of Piezo1 on T cells impairs anti-tumor immunity in vivo by hindering inflammatory T cell responses. We challenged mice with T cell Piezo1 deletion (P1KO) with tumor models dependent on T cells for immune rejection. P1KO mice had the more aggressive tumors, higher tumor growth rates and were unresponsive to immune-mediated therapeutic interventions. We observed a decreased CD4:CD8 ratio in both the secondary lymphoid organs and TME of P1KO mice that correlated inversely with tumor size. Poor $CD4^+$ helper T cell responses underpinned the immunodeficient phenotype of P1KO mice. Wild type $CD8^+$ T cells are sub-optimally activated in vivo with P1KO $CD4^+$ T cells, taking on a $CD25^{lo}PD-1^{hi}$ phenotype. Together, our results suggest that Piezo1 optimizes T cell activation in the context of a tumor response.

Introduction

Tumor-infiltrating lymphocytes (TILs) coordinate with other immune cells to induce cancer regression.[1] A bevy of evidence demonstrates that clinical outcomes are strongly correlated with the presence of TILs in the tumor microenvironment (TME).[2,3] Additionally, the quality of TILs has been recognized as a strong prognostic factor.[4–6] The presence of inflammatory T cell subsets (e.g., $CD4^+$ Th1, cytotoxic $CD8^+$) over anti-inflammatory subsets (e.g., $FoxP3^+CD4^+$ T_{regs}) results in better outcomes. However, how host factors contribute to the magnitude and quality of the TIL response is not well understood.

Cells of the hematopoietic system are unique in that they migrate throughout the body to exert their proper functionality. Flowing through vessels of different geometries, squeezing in between tight extracellular spaces, and crawling along stroma of varying compositions exposes immune cells to a barrage of mechanical stimuli. These cells sense these mechanical pressures and deformations and transduce them into signals that dictate the next sequence of biological events.[7] In recent years, this phenomenon of immunomechanobiology has garnered enthusiastic attention. Studies of the mechanosensory Piezo proteins have dominated inquiries. Between the two vertebrate members Piezo1 and Piezo2, Piezo1 is predominately expressed in non-neuronal tissues.[8–10] Piezo1 assembles into a homotrimeric propeller-like structure, with three blades surrounding a central cap.[11] Mechanical stimuli, such as membrane stretch, pries open the propellers away from the central cap, revealing a nonselective cation channel.

Recently, the roles of Piezo1 in the hematopoietic stem cell (HSC) lineages have been studied. Stimulation of Piezo1 on erythroblasts by the small molecule agonist Yoda1 results in increased binding to the adhesion molecules VCAM1 and fibronectin.[12] Among myeloid lineages, Piezo1 activation appears to potentiate inflammatory responses. In macrophages, Piezo1 stimulation enhances M1 inflammatory responses while reducing M2-like wound healing responses.[13] Dendritic cells (DCs) lacking Piezo1 skew T cells toward more T_{reg}-like and less Th1-like phenotypes[14] In T cells, Piezo1 stimulation potentiates T cell receptor (TCR) activation.[15] Under T_{reg} polarizing conditions, Piezo1 deficient $CD4^+$ T cells increased FoxP3 expression and induced less severe disease in an adoptive transfer model of experimental autoimmune encephalomyelitis (EAE).[10] Together, early results suggest that Piezo1 promotes inflammatory activation of T cells during antigenic challenge.

Despite these new insights, how Piezo1 on T cells affects anti-tumor immunity has not been examined. Here, we report that mice with CD4-driven genetic Piezo1 deletion (i.e., $CD4^+$ and $CD8^+$ T cells; P1KO mice) suffer from higher tumor burdens when challenged with a syngeneic murine

rhabdomyosarcoma (RMS) tumor, RMS 76–9. Tumor-bearing P1KO mice fail to respond to cryotherapy, which stimulates a potent inflammatory TME that results in tumor rejection in WT mice.[16] The P1KO antitumor response is characterized by a depressed $CD4^+:CD8^+$ T cell ratio in the tumor draining lymph node (tDLN) and TME that inversely correlates with tumor size. At the heart of this immunodeficiency is a deficit in antigen-specific T cell priming resulting in decreased helper $CD4^+$ T cell functional activity and subsequent blunting of cytotoxic $CD8^+$ T cell activation.

Materials and methods

Mice

As RMS 76–9 originated from male mice, to eliminate confounding issues related to H-Y dependent tumor rejection, only male mice were used for tumor experiments. CD4-Cre (Tg(CD4-Cre)1Cwi/BfluJ), Piezo1-floxed (B6.Cg-*Piezo1*$^{tm2.1Apat}$/J, #029213), B6 CD45.1 (B6.SJL-*Ptprc*^{a} *Pepc*^{b}/BoyJ, #002014), and male athymic nude mice (*Foxn1*^{nu}; #002019) were obtained from The Jackson Laboratory (Bar Harbor, ME). CD4-Cre/Piezo1$^{f/f}$ mice (P1KO) were generated by crossing CD4-Cre with Piezo1-floxed mice. OT1/CD4-Cre /Piezo1$^{f/f}$ (OT1KO) and OT2/CD4-Cre/Piezo1$^{f/f}$ (OT2KO) were generated by crossing P1KO mice with OT1 (JAX #003831) or OT2 (JAX #004194) mice, respectively. Confirmatory genotyping was achieved using polymerase chain reaction (PCR). Animals were housed, bred, and handled in the Animal Resource Center facilities at Case Western Reserve University according to approved protocols. All animal experiments were performed in 6- to 12-week-old animals with strict adherence to protocols approved by the Institutional Animal Care and Use Committee (protocol# 2015–0118) and performed in accordance with the guidelines of the American Association for Accreditation of Laboratory Animal Care and the NIH.

Cells

Murine RMS WT (RMS 76–9)[17,18] (provided by C. Mackall, Stanford University) was stably transfected with a plasmid encoding soluble ovalbumin (OVA) co-expressed with eGFP via an IRES sequence to generate the RMS-OVA cell line (pOVA-IRES2-EGFP I.2). After fluorescence-activated cell sorting (FACS) to enrich for GFP$^+$ clones, the RMS-OVA cell line was tested for OVA peptide expression via flow cytometry using an antibody specific for the OVA$_{257–264}$ (SIINFEKL) sequence in the context of H2-K^b (25-D1.16, BioLegend). Murine medulloblastoma (MM1),[19] RMS WT and RMS-OVA cell lines were cultured in RPMI 1640 media supplemented with 10% FBS, L-glutamine, sodium pyruvate, HEPES, non-essential amino acids, and penicillin/streptomycin.

T cells specific for OVA$_{257–264}$ /H2-K^b or OVA$_{323–339}$/I-A^b were isolated from the spleens and LNs of 6- to 12-week-old OT1 or OT2 mice, respectively. Positive sorting via magnetic bead selection kits from Miltenyi Biotec (Paris, France) yielded CD8$^+$ OT1 and CD4$^+$ OT2 T cells with purities above 90%. Both OVA-specific and polyclonal CD4$^+$ and CD8$^+$ T cells were cultured in RPMI 1640 media supplemented with 10% FBS, L-glutamine, sodium pyruvate, HEPES, non-essential amino acids, penicillin/streptomycin, and β-mercaptoethanol.

In vivo tumor growth and immune cell isolation

1×10^6 RMS 76–9 cells were injected s.c. in the flanks of 6- to 12-week-old male mice. Tumor sizes were assessed twice weekly using a caliper, and volumes were calculated according to the equation $V = \frac{1}{2} (D \times d^2)$, where D and d are the lengths of the long and short tumor dimension, respectively. Mice were euthanized, and tumors were removed, weighed, and digested in 1 mg/mL Collagenase D and 20 U/mL DNase1. Single-cell suspensions were obtained following sequential passes through 70 μm and 40 μm cell filters with FACS buffer (0.5% FBS and 0.5% 0.5 M EDTA in PBS). tDLNs and spleens were isolated, smashed, and filtered through 40–70 μm filters. Red blood cells were removed using an ammonium chloride lysis solution.

Flow cytometry

Analysis of cell surface markers, intracellular cytokines, and transcription factors was conducted using the CytoFLEX flow cytometer and data analyzed using the CytExpert software (Beckman Coulter, Pasadena, CA, USA). 100 μL of cell suspension was incubated with 1.25 μg/mL rat anti-mouse CD16/32 (clone 93; BioLegend) for 30 minutes on ice, followed by surface staining using the antibodies listed in Supplemental Table 1. Fixation and permeabilization were achieved using the eBioscience Intracellular Fixation and Permeabilization kits. For intracellular cytokine staining, polyclonal T cells were stimulated overnight with 1 μg/mL anti-CD3e (145-2C11; BD) and 0.5 μg/mL anti-CD28 (37.51; BD) at 37°C. Ovalbumin (Ova)-restricted T cells were incubated with 1 μg/mL OVA$_{257–264}$ and/or OVA$_{323–339}$ peptides for 4 hours. Four hours prior to staining cells were incubated with BioLegend Cell Activation Cocktail with Brefeldin A (#423304). Cells were washed in FACS buffer prior to acquisition. Where appropriate, the number of events of interest was extrapolated to whole tissues.

In vitro T cell calcium assay

Polyclonal CD4$^+$ and CD8$^+$ T cells were isolated from the spleens of 6- to 12-week-old WT and P1KO mice. After a 48 h incubation with anti-CD3/CD28 antibodies, T cells were incubated with 5 μM Fluo4-AM for 15 min at 37°C. T cells were then resuspended in a solution containing 1:2000 DMSO +2 mM CaCl$_2$ or 25 μM Yoda1 + 2 mM CaCl$_2$ and immediately assessed for Fluo4 positivity via flow cytometry.

Tumor cryoablation

Cryoablation was performed using the ProSense Cryosurgical System (IceCure Medical Ltd) via a cryoprobe delivering liquid nitrogen at a temperature of −196°C. When tumor volumes were approximately 100 mm^3, mice were anesthetized with 2–3% isoflurane and the cryoprobe was placed directly on the tumor mass percutaneously. Cryoablation was performed at

a high freezing rate (~1.67 mm^3 tumor tissue/second) with each tumor undergoing three cycles of freezing (1-minute freeze and 3-minute thaw).

In vivo proliferation assay

Naïve CD8$^+$ OT1 and CD4$^+$ OT2 T cells were incubated with 5 μM CFSE for 10 minutes at 37°C. Labeled OT1 and OT2 cells (4 × 10^6 total; 1:1 ratio OT1:OT2) were injected intravenously (i.v.) into 6- to 12-week-old naïve male and female CD45.1 mice. Twenty-four hours later, recipient mice were immunized with 50 μL of whole ovalbumin (50 μg) and CpG (20 μg) suspended in Alum. Proliferation was assessed 72 hours later by harvesting DLN and spleens followed by flow cytometry on CD45.2$^+$CD45.1$^-$ cells.

In vitro cytotoxic lymphocyte (CTL) assay

Splenocytes were harvested from 6- to 12-week-old naïve OT1 male and female mice and plated at 1×10^6 cells/mL with 1 μg/mL SIINFEKL and 100 U/mL recombinant mouse IL-2 (BioLegend). Culture media was replaced on day 3. On day 5, cells were harvested and incubated with RMS-OVA cells at various effector:target ratios for 4 hours. Target cell viability was assessed by incubation with 50 μg propidium iodide followed by flow cytometry, gating on GFP$^+$ tumor cells.

In vitro soluble factor vs. direct cell–cell contact-dependent activation assay

Polyclonal CD4$^+$ T cells were harvested from 6- to 12-week-old naïve male and female WT or P1KO mice. Following 72 hours of anti-CD3/CD28 stimulation, CD4$^+$ T cells were either added to 3 μm polycarbonate membrane transwell inserts or directly to cultures containing 5×10^4 RMS-OVA, 1×10^6 irradiated CD45.1 splenocytes, and 1×10^6 naïve, CFSE-labeled CD8$^+$ OT1 WT T cells. After an additional 72 hours, cells were harvested and processed for analysis on flow cytometry.

Quantitative PCR

TRIZOL Reagent was used for RNA extraction and isolation. Following RNA quantification, reverse transcription (RT) of 0.5–1 μg of total RNA was performed using the High-Capacity cDNA Reverse Transcription kit (Thermo Fisher Scientific #4368814). Real-Time quantitative PCR was carried out on the resulting cDNA using Bullseye EvaGreen qPCR Master Mix (MIDSCI, Fenton, MO) or TaqMan Gene Expression Master Mix (ThermoFisher Scientific, Waltham, MA) on the BioRad CFX96 Real-Time System to determine transcript expression of *Piezo1* (Fw: 5'-TTGACCCTGCCAACTGGTTT -3'; Rv: 5'-GCCTCAAACACCAGCAACAG-3') and *Piezo2* (TaqMan Gene Expression Assay, Mm01265858_m1). *Cyc1* (Fw 5'- CTGCCACAGCATGGATTATG-3'; Rv: 5'- CATCAT CATTAGGGCCATCC-3') served as a reference gene. Analysis was performed using the delta-delta C$_T$ ($2^{-\Delta\Delta CT}$) method.

Quantification and statistical analysis

All statistical analyses were calculated using GraphPad Prism software. *P*-values calculated either using unpaired Student's t-test (two groups) or one-way ANOVA with Tukey's multiple comparisons testing (three or more groups).

Results

Tumor-bearing P1KO mice have a depressed CD4$^+$:CD8$^+$ T cell ratio in the tDLN and TME

Human RNA sequencing data[20] reveal that Piezo1 transcripts increase following T cell activation and differentiation into effector states (Figure 1a). As global deletion of Piezo1 is embryonically lethal,[21] we employed a previously described T cell-specific knockout model (P1KO) by crossing CD4-Cre mice with mice containing flox sequences on the *Piezo1* gene (Piezo1$^{f/f}$),[10] resulting in both CD4$^+$ and CD8$^+$ T cells that are deficient in functional Piezo1 expression (Figure 1b,c). No compensatory expression of *Piezo2* was observed in either naïve or activated P1KO T cells (Figure S1a,b). As both T cell subsets play central roles in tumor clearance,[3,22–24] we sought to assess the response of P1KO mice *to in vivo* tumor challenge. We inoculated mice with RMS 76–9, a murine model of embryonal RMS,[17,18] and monitored their growth. P1KO mice demonstrated increased tumor growth kinetics and size (Figure 1d). We harvested both tumor and tDLN 2 weeks post inoculation and assessed the immune cell status using flow cytometry (Figure S2a). Frequencies and numbers of leukocytes were unchanged in the P1KO TME (Figure S2b), as were the total numbers of both CD4$^+$ and CD8$^+$ T cells in the tDLN (Figure S2d,f) and TME (Figure S2c,e,g). Relative proportions of myeloid cell populations were also unchanged in the P1KO TME (Figure S3a,b). Interestingly, we observed a drastically reduced CD4$^+$ to CD8$^+$ T cell ratio in both the tDLN and TME in P1KO versus WT mice (Figure S2h,i).

To further explore the relevance of a decreased CD4$^+$:CD8$^+$ T cell ratio in P1KO mice, we analyzed tumor volumes as a function of either the CD4$^+$:CD8$^+$ T cell ratio, total CD4$^+$ T cell count, or total CD8$^+$ T cell count. In the tDLN, the CD4$^+$: CD8$^+$ T cell ratio most strongly inversely correlated with tumor size ($R^2 = 0.294$), whereas the individual CD4$^+$ or CD8$^+$ T cell counts had very weak inverse correlations ($R^2 = 0.084$ and <0.001, respectively; Figure 1e–g). A similar pattern was seen in the TME with an inverse correlation between CD4$^+$:CD8$^+$ ratios and tumor volume ($R^2 = 0.304$). However, unlike in the tDLN, the TME CD4$^+$ T cell counts demonstrated similar inverse correlation ($R^2 = 0.250$), while CD8$^+$ T cell counts showed a poor correlation with tumor size (Figure 1h–j).

To ensure that our observed results are characteristic of the general tumor response in P1KO and not specific to the RMS model, we challenged P1KO mice with MM1, a syngeneic murine medulloblastoma model.[19] As seen with RMS, MM1 demonstrated a trend in enhanced growth kinetics in P1KO mice compared to WT (Figure S4a,b). P1KO mice also had reduced tDLN CD4$^+$:CD8$^+$ T cell ratios, which were inversely correlated with tumor size
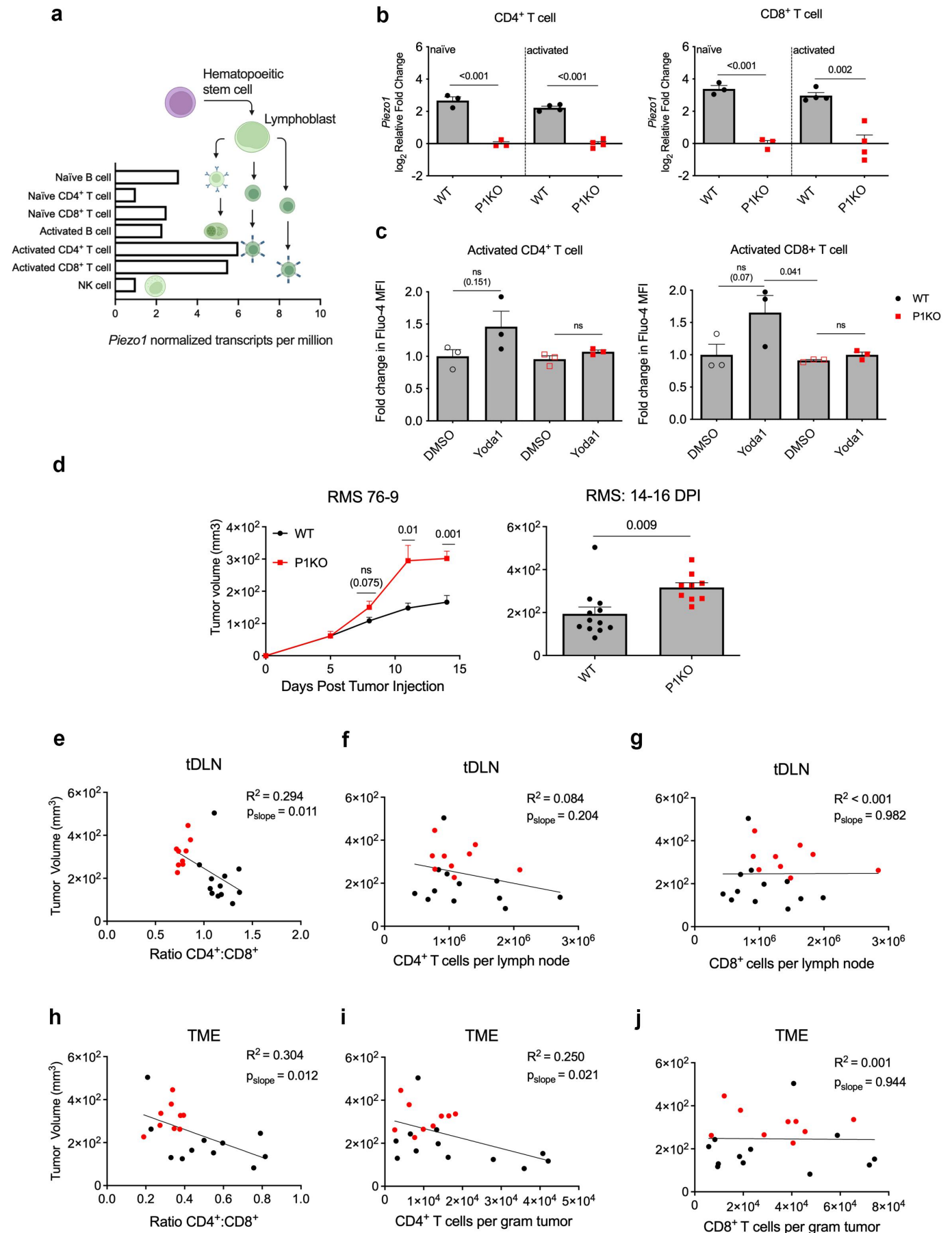
Figure 1. Phenotype of tumor-bearing P1KO mice. (a) RNA sequencing data from the human protein atlas demonstrating normalized PIEZO1 expression among lymphocyte subsets. (b) Transcripts of *Piezo1* in CD4$^+$ (left) and CD8$^+$ (right) T cells after 3-day stimulation with anti-CD3/CD28 antibodies were assessed using

(Figure S4c,e,g). Like RMS, MM1 tDLN and TME CD4$^+$ T cell counts correlated inversely with tumor size (Figure S4d,f,h,j). Taken together, these results demonstrate that T cell specific Piezo1 deletion renders mice susceptible to enhanced tumor growth and perturbed T cell compartments.

Previously published studies have demonstrated no differences in the proportions of T cells in various tissues between WT and P1KO mice.[10] Ingress and egress of naïve T cells into LNs were also unaffected.[10] These results suggest that the perturbed T cell compartments in P1KO tDLN and TME reflect a possible Piezo1-associated deficit in CD4$^+$ T cell activation, function or persistence.

P1KO mice fail to respond to immunogenic tumor challenge

RMS 76–9 induces a potent immunosuppressive TME that overwhelms the endogenous immune response over extended time periods (Figure 2a)[25] To mitigate this, we employed cryoablation, which induces immunogenic death and tumor clearance in a CD4$^+$ and CD8$^+$ T cell-dependent matter.[16] CD8 depletion yields cryoablated tumors no different in size than unablated tumors, while CD4 depletion results in partial therapeutic efficacy to cryoablation. Cryoablation in P1KO mice yielded tumors that initially regressed but then rebounded 12 days after the procedure (Figure 2a), with only 20% tumor-free survival compared to 80% of WT mice receiving cryoablation (Figure 2b), an observation very similar to RMS response to cryoablation in WT mice depleted of CD4$^+$ T cells.[16] Interestingly, the overall CD45$^+$ leukocyte and CD3$^+$ T cell infiltration were similar in the TME (Figure 2c,d) and the tDLN (Figure 2e). Next, we assessed the quality of the effector T cells that may account for the ineffective response in P1KO mice. Both interferon gamma (IFNγ) and CD25 on tDLN CD8$^+$ T cells were increased in cryoablated versus non-cryoablated WT mice; however, neither marker was appreciably different in cryoablated versus non-cryoablated P1KO mice (Figure 2f,g). tDLN CD4$^+$ T cells in tumor-bearing P1KO mice exhibited higher PD-1 expression on day 14–16, which then normalized by day 22 (Figure S5a,b). In contrast, tDLN CD8$^+$ T cells in tumor-bearing P1KO mice exhibited persistently higher PD-1 expression (Figure S5c,d). Taken together, these results suggest that cryoablation induces immune rejection in RMS 76–9 by enhancing CD8$^+$ T cell activation, a process dependent on T cell expression of Piezo1.

Next, we interrogated the quality of the CD4$^+$ T cell pool[23,24] and were surprised to find a trend toward increased CD25 expression among CD4$^+$ T cells in cryoablated P1KO mice when compared to WT (Figure 2h). This led us to consider the possibility of increased CD4$^+$ regulatory T cells (T$_{reg}$), as deletion of Piezo1 on CD4$^+$ T cells has been reported to result in the expansion of the T$_{reg}$ pool.[10] We found similar frequencies of FoxP3$^+$ effector CD4$^+$ T cells in the tDLN and TME 2 weeks after cryoablation (Figure 2 l,j). In MM1, we also fail to observe increase T$_{reg}$ generation in tumor-bearing P1KO mice (data not shown). Our results suggest that, contrary to findings in autoimmune models, Piezo1 does not play a significant role in T$_{reg}$ generation during tumor challenge *in vivo*.

Enhanced tumor growth in P1KO mice is due to Piezo1-deficient T cells and not CD4$^+$ myeloid cells

Recent studies have shown that Piezo1 deficiency on CD11c$^+$ DCs increases tumor burden secondary to expansion of the T$_{reg}$ CD4$^+$ T cell pool during antigenic priming.[14] We considered the possibility that the results observed in P1KO mice may be due to Piezo1 deletion on certain subsets of DCs, macrophages, and monocytes expressing CD4.[26,27] To more precisely assess the role of T cell-specific Piezo1, we crossed P1KO mice with OT1 and OT2 mice to generate ovalbumin-reactive, Piezo1-deficient CD8$^+$ and CD4$^+$ T cells (OT1KO and OT2KO, respectively). Athymic nude mice were inoculated with RMS 76–9 expressing ovalbumin (RMS-OVA). One week later, a 1:1 ratio of OT1KO and OT2KO T cells was adoptively transferred followed by cryoablation 24 hours later (Figure 3a, S6a). Mice receiving WT OT1/OT2 T cells experienced a trend showing reduced tumor growth compared to control mice or mice receiving both OT1KO and OT2KO T cells (Figure 3b). Frequencies of IFNγ$^+$ OT1KO T cells were decreased in the tDLN and TME (Figures 3c and S6b). The CD25$^+$FoxP3$^+$ T$_{reg}$ pools were surprisingly reduced in the DLN of P1KO mice, although similar frequencies were observed in the TME (Figures 3d and S6c). Similarly, there were no discernable differences in the naïve, T$_{cm}$, or T$_{em}$ cells in the tDLN (Figure 3e,f and S6d) or TME (data not shown) between WT and P1KO mice. These results confirm that the T cell phenotype we observe in tumor-bearing P1KO mice is due to the absence of Piezo1 on CD3$^+$ T cells, and that Piezo1 does not impact the frequency of the memory T cell pool during tumor challenge.

Piezo1 expression on CD8$^+$ T cells is dispensable for antigen-induced proliferation and cytotoxicity

We sought to distinguish CD8$^+$ T cells or CD4$^+$ T cells dependency on Piezo1 for their functional activation. In both immunocompetent and nude murine tumor models, we observed decreased IFNγ expression in Piezo1-deficient CD8$^+$ T cells in the tDLN, a major site of priming naïve, tumor-antigen specific

---

RT-qPCR. (c) Polyclonal CD4$^+$ (left) and CD8$^+$ (right) T cells were subject to anti-CD3/CD28 stimulation for 48 hours before being loaded with Fluo4-AM. Cells were briefly exposed to 25 μM Yoda1 and Fluo4 fluorescence was assessed by flow cytometry. (d) Tumor growth curve of RMS 76–9 bearing mice (left) with tumor volume on days 14–16 post tumor injection (DPI) (right). Day 14–16 tumor volumes as a function of the CD4$^+$:CD8$^+$ T cell ratio (e,h), CD4$^+$ T cell count (f,i) or CD8$^+$ T cell count (g,j) in tumor draining lymph node (tDLN) and tumor microenvironment (TME), respectively. R^2 and *p*-value of slope calculated using simple linear regression analysis. Data shown pooled from at least 2–3 independent experiments. Plots of group means, standard error, and associated *p*-values between groups. ns = not statistically significant at an alpha of 0.05.
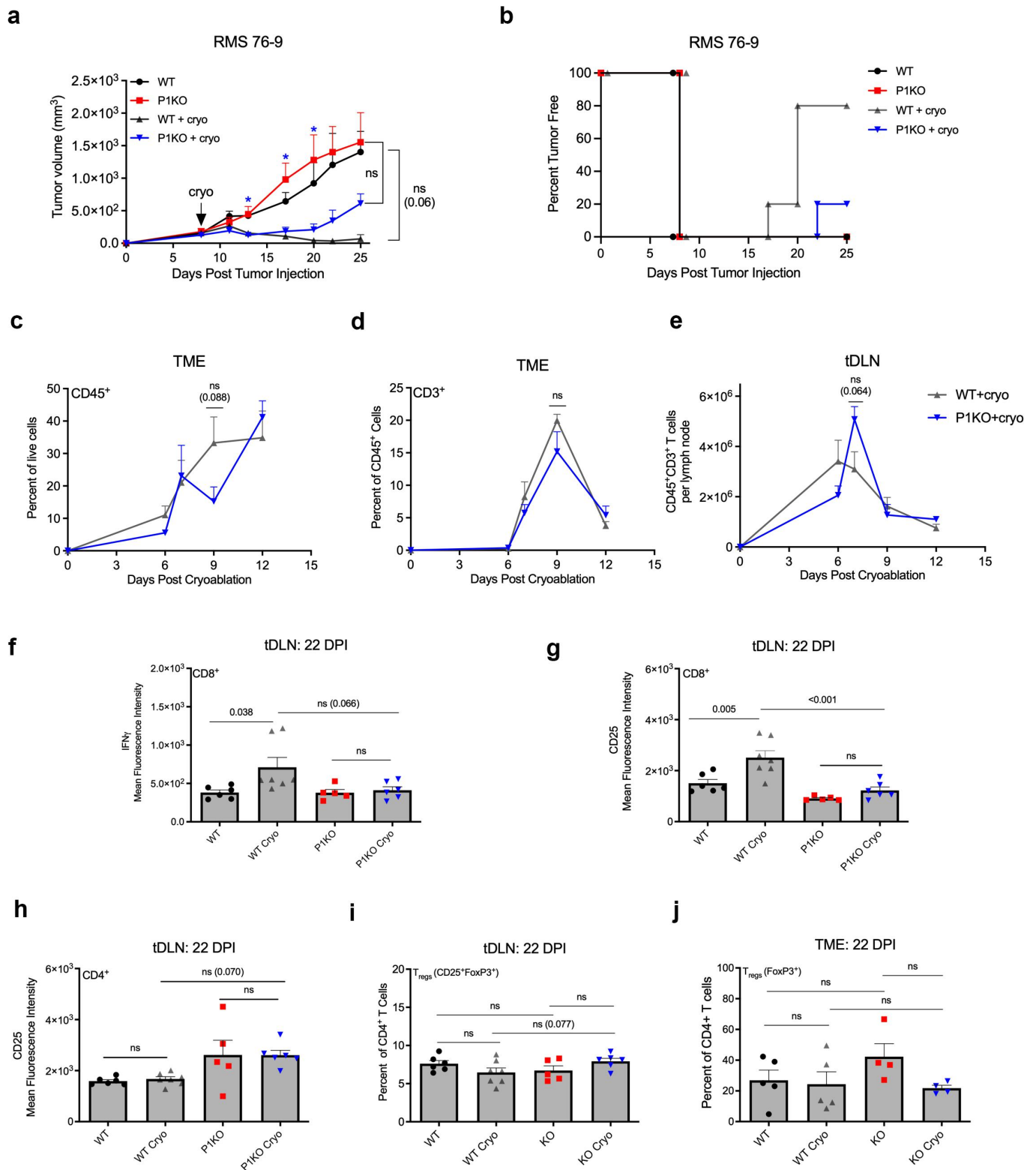
Figure 2. Piezo1 deficient mice fail to respond to immunogenic tumor challenge. (a) 1×10^6 RMS were inoculated s.c. In WT or P1KO mice. Tumors were cryoablated on day 8 (arrow) and their volumes were measured following cryoablation. Blue star (*) indicates a *p*-value <0.05 obtained from one-way ANOVA testing between P1KO and P1KO+cryo groups, with an alpha of 0.05. (b) Kaplan–Meier curve for tumor-free survival among different groups of mice (*n* = 4–5 mice per group). (c) Frequencies of CD45+ and CD3+CD45+ cells gated on live singlets from tumor samples at various timepoints following cryoablation. (d) Total CD3+ T cell counts from the tumor microenvironment (TME) and (e) tumor draining lymph node (tDLN) following cryoablation. Two weeks following cryoablation CD3+CD8+ T cells from the tDLN were examined for expression of IFNγ (f) and CD25 (g) as determined by mean fluorescence intensity (MFI). CD3+CD4+ T cells were also examined for CD25 expression (h). Frequency of FoxP3 on CD4+ T cells taken from the tDLN (i) or TME (j) 2 weeks following cryoablation. Plots of group means, standard error, and associated *p*-values between groups. ns = not statistically significant at an alpha of 0.05. DPI = days post tumor injection.

CD8^{+} T cells into effector CTLs. To determine the role of Piezo1 during CTL generation, we adoptively transferred CFSE-labeled OT1WT or OT1KO cells into CD45.1 congenic mice and challenged them 1 day later with ovalbumin. Immunization site DLN (Figure 4a,b left) and spleen (data not shown) showed similar cell division kinetics between OT1WT and OT1KO T cells, as well as similar number of total CD8^{+} T cells (Figure 4b, right), indicating that Piezo1

does not significantly influence antigen-induced proliferation in CD8^{+} T cells. Next, we analyzed the effector function of OT1KO CD8^{+} T cells. *In vitro* SIINFEKL-primed OT1KO splenocytes were incubated with RMS-OVA target cells to assess cytotoxicity. At all effector:target ratios, no significant difference in cytotoxicity was observed between OT1WT or P1KO splenocytes (Figure 4c), confirming that Piezo1-deficient CD8^{+} effector CTL function remained intact.
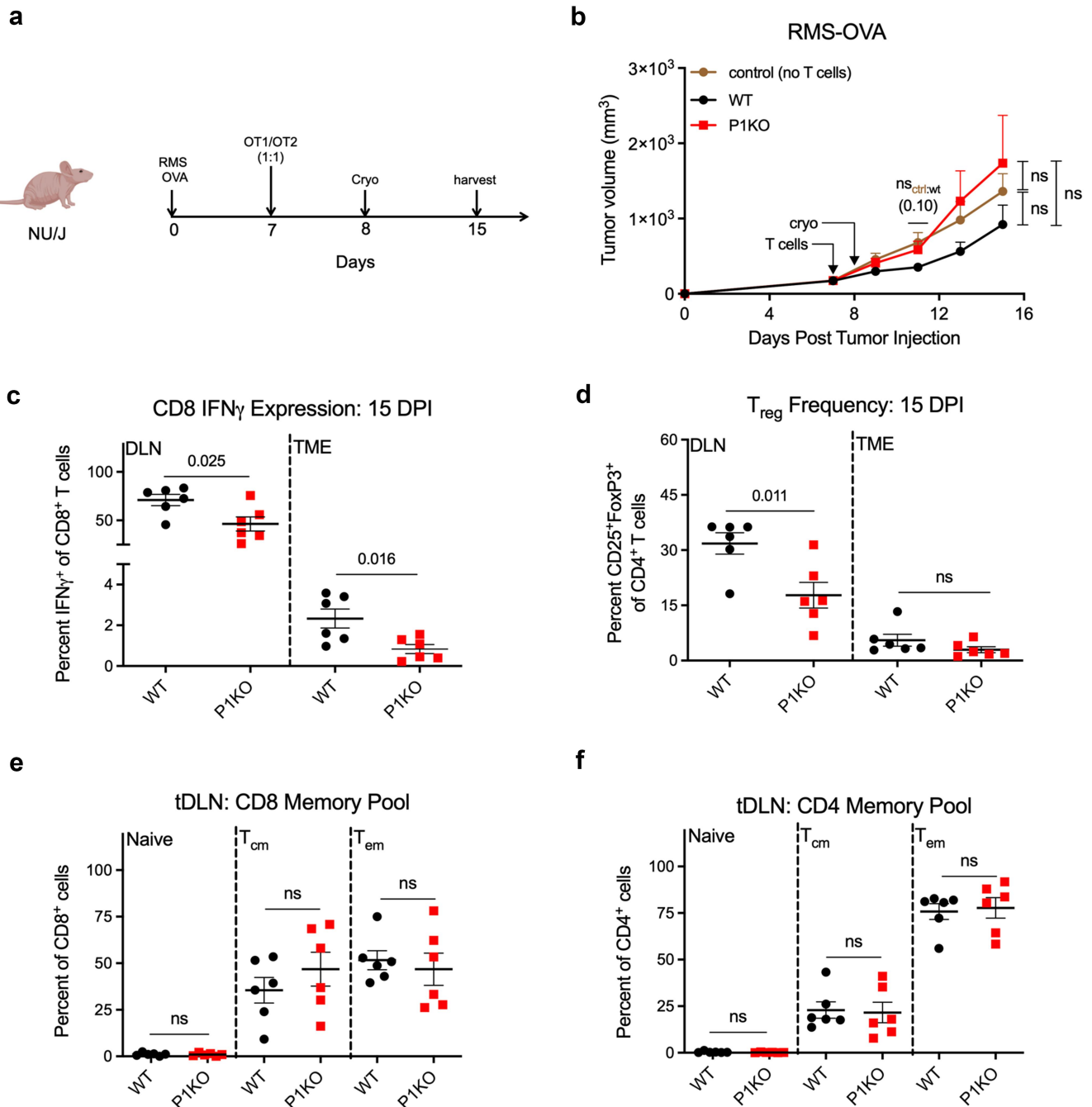
Figure 3. Piezo1 depletion in T cells underlies the immune dysfunction observed in CD4-Cre/Piezo1[f/f] mice. (a) Schematic of nude mouse tumor challenge. A 1:1 ratio of OT1:OT2 T cells (WT) or OT1KO:OT2KO T cells (P1KO) were adoptively transferred into nude mice at day 7 post s.c. tumor injection, with cryoablation 24 hours later. (b) Tumor growth kinetics of RMS 76–9 transfected with ovalbumin (RMS-OVA) in nude mice. Control group received no T cells. $ns_{ctrl:wt}(x)$ indicates the *p*-value obtained from means testing between control and WT groups. (c) Frequencies of IFNγ^{+}CD8^{+} (c) and CD25^{+}FoxP3^{+}CD4^{+} (d) T cells from harvested tumor draining lymph nodes (tDLN) and tumor samples (TME). Antigen experienced memory populations among CD8^{+} (e) and CD4^{+} (f) T cells in the tumor draining lymph node (tDLN). Naïve = CD44^{−}CD62L^{+}; T_{cm} = CD44^{+}CD62L^{+}, T_{em} = CD44^{+}CD62L^{−}. Plots of group means, standard error, and associated *p*-values between groups. ns = not statistically significant at an alpha of 0.05. DPI = days post tumor injection.
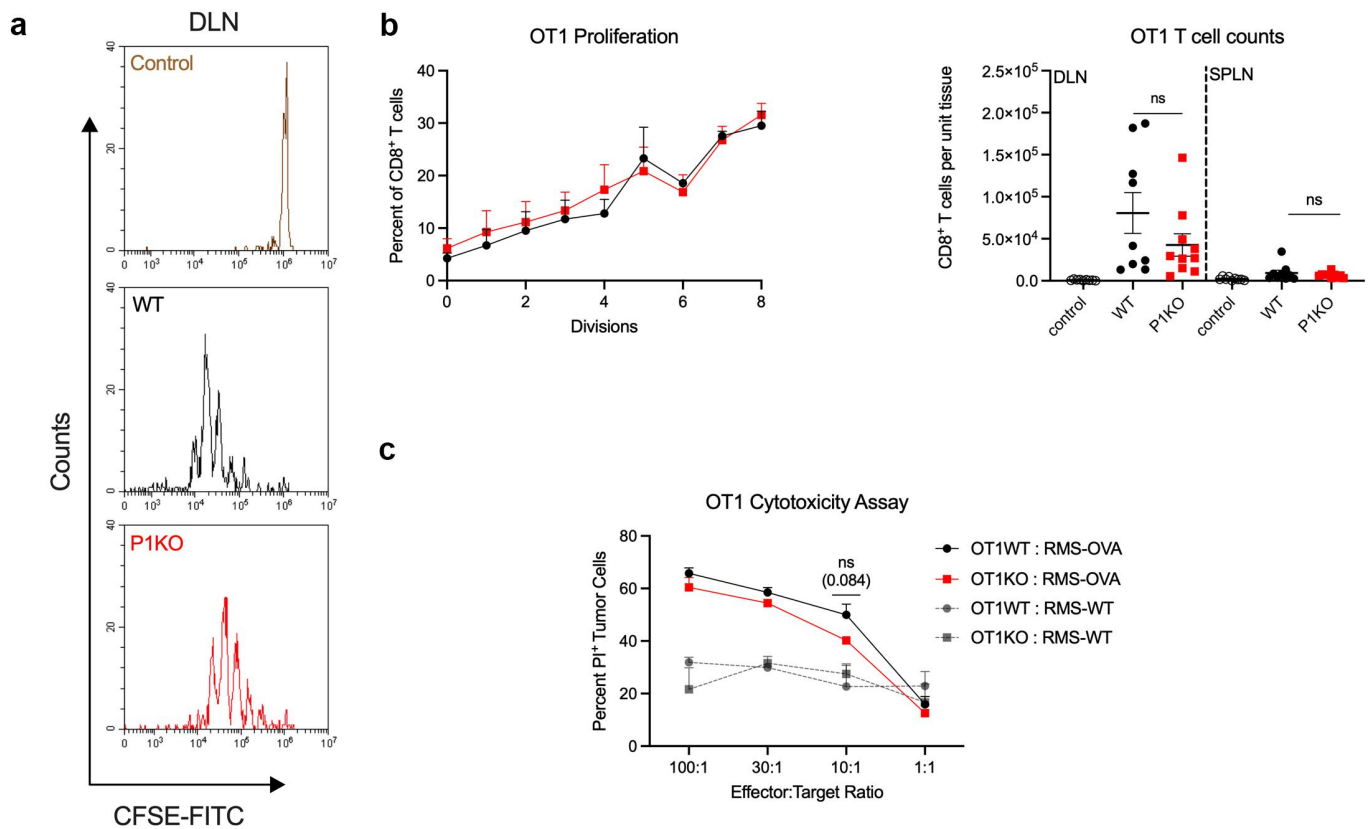
Figure 4. CD8⁺ T cell Piezo1 expression is dispensable for CTL immunity. (a) CFSE dilution peaks of adoptively transferred OT1WT (black), P1KO (red), or control OT1WT (brown) T cells 72 hours after host vaccination with ovalbumin (PBS; control). (b) Plot of the percentage of transferred OT1 T cells having gone through $n = x$ rounds of divisions. Percentages obtained by calculating the area under the curve of an individual CFSE dilution peak. (B, right) total OT1 counts in draining lymph nodes (DLN) and spleen (SPLN). (c) Propidium iodide (PI) staining of RMS-OVA tumor cells following incubation with activated OT1 splenocytes at various splenocyte-to-tumor ratios (effector:target ratio); $n = 3$ mice per group. Plots of group means, standard error, and associated p-values between groups. ns = not statistically significant at an alpha of 0.05.

Piezo1 on CD4⁺ T cells directs optimal CD8⁺ T cell activation

The absence of Piezo1 on both CD4⁺ T cells and CD11c⁺ DCs leads to CD4⁺ T_{reg} pool expansion in prior studies.[10,14] We examined whether this occurs during antigen-specific priming. We adoptively transferred CFSE-labeled OT2WT or OT2KO T cells with CFSE-labeled OT1WT T cells into naïve CD45.1 mice, immunized them with ovalbumin protein, then harvested tissues for analysis (Figure 5a). OT1WT T cells showed similar proliferation (Figure 5b,c, left) and abundance (Figure 5c, right) in the DLN and spleen when co-transferred with either OT2WT or OT2KO T cells. OT2KO T cells proliferated at a slightly lower rate than OT2WT T cells, having gone through one fewer round of division at the time of harvest (Figure 5b,d, left). However, the total number (Figure 5d, right) of OT2WT and OT2KO in the DLN and FoxP3 positivity (Figure 5e) were similar. Curiously, CD25 as well as IFNγ and Granzyme B (Gzmb) were decreased in OT1WT T cells that were co-transferred with OT2KO T cells (Figure 5f–h). More strikingly, a similar pattern was seen in the host resident CD45.1⁺CD45.2⁻CD8⁺ pool (Figure 5,i,j).

Based on data above, we hypothesized a role for Piezo1 in influencing CD4⁺ T cell interaction with cognate antigen-presenting cell (APC). Classically, conventional DCs (cDCs) can be characterized into cDC1 or cDC2 subsets that efficiently present antigen to CD8⁺ and CD4⁺ T cells, respectively.[28–30]

CD4⁺ T cells are necessary to direct optimal expansion of CTL pools during antigen challenge,[31–33] and CD4⁺ T cell help of CD8⁺ T cells is contingent on DC licensing by CD4⁺ T cell via CD40-CD40L interactions,[34] resulting in upregulation of CD80 and pro-inflammatory cytokines in DCs.[35,36] Surprisingly, we observed increased CD40L expression on *in vitro* activated CD4⁺ P1KO T cells (Figure S7a). We then assessed cDCs in ovalbumin immunized mice following adoptive transfer of OT1WT and OT2KO T cells. No differences were seen in the frequency, number, CD40, or CD80 levels on cDCs harvested from DLNs (Figure S7b–d). The frequencies of cDC1s and cDC2s and their activation status were similar (Figure S7e–g).

Next, we assessed the tDLN and TME of tumor-bearing WT and P1KO mice for changes in cDC frequencies. Tumor-bearing P1KO mice showed increased percentages and total numbers of cDCs in the tDLN (Figure S7h) but not in the TME (Figure S7i). We concluded that Piezo1 expression on CD4⁺ T cells facilitates optimal generation of the CTL pool in an APC-independent fashion.

Piezo1-associated release of soluble factors regulates CD8⁺ T cell activation in the context of CD4 help

CD4⁺ T cell coordination of CD8⁺ T cell activation involves both targeted cytokine release and the engagement of
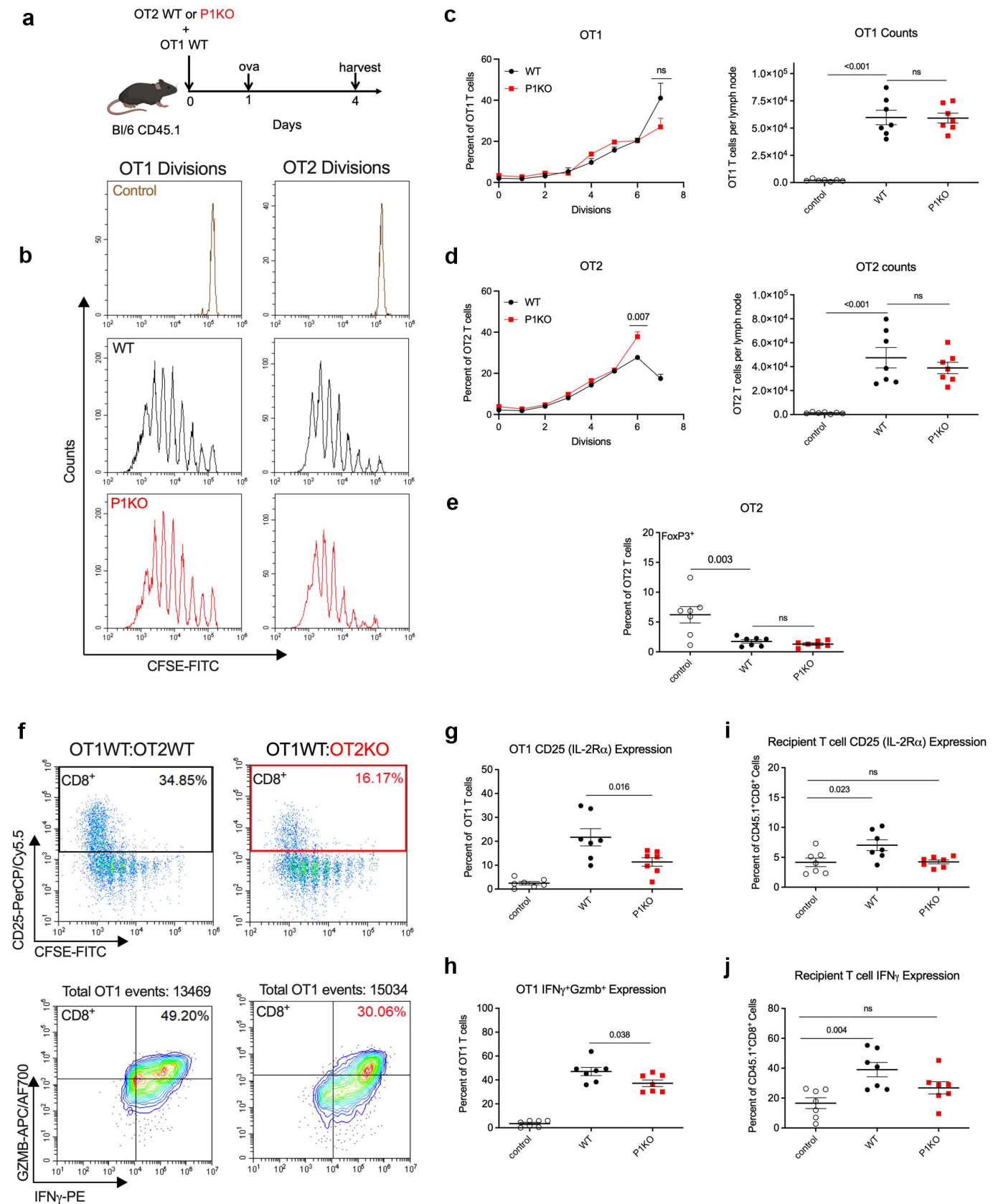
Figure 5. Piezo1 on CD4$^+$ T cells directs optimal CD8$^+$ T cell activation. (a) Schematic of *in vivo* T$_{reg}$ suppression assay. A 1:1 ratio of OT1WT and OT2WT or OT2KO T cells were transferred into CD45.1 donor mice, with subsequent ovalbumin immunization. (b) CFSE dye dilution peaks of adoptively transferred OT1 (left) T cells into donor mice receiving OT2 WT but sham immunization with saline (control, brown), OT2WT (black) or OT2KO (red) with ovalbumin immunization. (c) Quantification of divisions of OT1 T cells (left) and total counts (right) of transferred OT1 T cells in the ovalbumin immunization site draining lymph node. (d) Quantification of divisions (left) and total counts (right) of OT2 T cells. (e) Expression of FoxP3 on draining lymph node OT2 T cells. (f) Flow analysis of OT1WT T cells co-transferred with either OT2WT (left, black) or OT2KO (right, red) T cells. Gating for CD25$^+$ (top) and IFNγ$^+$Gzmb$^+$ (bottom) OT1s. (g) Quantification of CD25 positive and IFNγ$^+$Gzmb$^+$ double positive (h) OT1 populations. (h) Percent positive expression of CD25 (i) IFNγ (j) among recipient CD45.1$^+$CD8$^+$ cells in the immunization site draining lymph nodes. Plots of group means, standard error, and associated *p*-values between groups.

reciprocal receptor pairs.[31–33,37] We sought to clarify which factor may be more important for the generation of CTL immunity by assessing the activation of CD8^{+} T cells during contact or contactless CD4 help. We utilized naïve OT1WT T cells cultured with activated CD4^{+} T cells directly or via a transwell membrane insert in the presence of Ova-expressing tumor cells (Figure 6a). OT1s in all groups generally proceeded through cell division at a similar rate (Figure 6b,c). Most strikingly, OT1s exposed to P1KO CD4 help through either a transwell or direct cell–cell contact exhibited blunted upregulation of CD25 in later rounds of division (Figure 6d,e). This result strongly suggests that Piezo1-associated CD4^{+} T cell secretion of soluble factors drives optimal CD4-mediated CD8^{+} T cell CD25 expression, mirroring results observed *in vivo* (Figures 2g and 5f,g).

We further probed this CD25^{+} OT1 population for additional markers for clues regarding their functional status. CD25^{+} OT1s exposed to P1KO CD4^{+} T cells through either a transwell or direct cell–cell contact demonstrated increased PD-1 expression (Figure 6f), mirroring the sustained expression of PD-1 seen on CD8^{+} T cells activated in the presence of P1KO CD4^{+} T cells *in vivo* (Figure S5c,d). TCR-mediated stimulation was not impacted by the Piezo1 status or direct contact by CD4^{+} T cells, as evidenced by similar CD44 (Figure 6g) and TNFα/IFNγ/Gzmb expressions (Figure 6h) among OT1s in various experimental groups.

Discussion

The mechanosensitive Piezo1 channel is highly expressed on HSC lineages and modulates various immune cell processes.[7,12,13,21] Prior studies suggest that Piezo1 stimulation in T cells is pro-inflammatory. On human T cells, Piezo1 stimulation synergistically potentiates TCR signaling and results in enhanced activation.[15] Murine models of autoimmunity demonstrate diminished disease severity with T cell-specific Piezo1 deletion.[10] Our current studies sought to define a role for Piezo1 on both CD4^{+} and CD8^{+} T cells in a tumor model. P1KO mice experienced enhanced tumor growth *in vivo* with two distinct tumor types, RMS and MM1 (Figure 1d and S4b). Cryoablation, known to induce a potent T cell-dependent tumor rejection,[16] failed to induce an effective anti-tumor response in P1KO mice (Figure 2a,b). Underlying this ineffective response is a depressed CD4^{+}: CD8^{+} T cell ratio in the tDLN and TME (Figure 1e,h and S2h,i), the significance of which is not immediately apparent. However, several clinical studies suggest an association of this ratio with positive clinical outcomes. Shah *et al.*[38] reported that a high CD4^{+}:CD8^{+} TIL ratio, not the number of individual CD4^{+} or CD8^{+} T cells, is associated with overall survival in patients with squamous cell carcinoma of the cervix. In triple-negative breast cancer, a CD4^{+}:CD8^{+} ratio >1 is associated with increased overall survival.[39] In the HIV/AIDS cohort, a depressed CD4^{+}:CD8^{+} ratio is associated with an increased cancer risk independent of either CD4^{+} or CD8^{+} T cell counts.[40] In the context of normal CD4^{+} counts, a depressed CD4^{+}:CD8^{+} ratio may be indicative of CD8^{+} T cell exhaustion.[41,42] Consistent with these observations, we found elevated levels of the exhaustion marker PD-1 on P1KO CD8^{+}

T cells in the tDLN (Figure S5c,d), with diminished CD25 and IFNγ expression following cryoablation (Figure 2f,g).

As previous reports suggest enhanced T$_{reg}$ generation in mice with Piezo1 deletion in either the T cell or DC compartments,[10,14] we investigated whether a similar response could explain the immune dysfunction seen in tumor-bearing P1KO mice. However, we failed to observe increased expression or number of CD25^{+}FoxP3^{+}CD4^{+} T cells in the DLN or TME in P1KO mice (Figures 2i and 3c). Enhanced T$_{reg}$ responses were also not observed in OT2KO T cells following ovalbumin vaccination. The FoxP3^{+} pool was unchanged between OT2WT and OT2KO T cells (Figure 5e), and OT1WT T cells proliferated similarly in the presence of either OT2KO or OT2WT T cells (Figure 5c). Despite previous findings, the immune dysfunction observed in tumor-bearing P1KO mice cannot be explained by an expanded T$_{reg}$ pool.

Rather, our investigations reveal a role for CD4 Piezo1 in facilitating CD4^{+} T cell helper responses for optimal CD8^{+} T cell activation. In response to ovalbumin vaccination, OT1WT T cells co-transferred with OT2KO T cells have blunted activation (Figure 5f,g,h). Host polyclonal CD8^{+} cells in the DLN also exhibited decreased activation (Figure 5i,j), suggesting decreased helper CD4^{+} T cell activity. While CD4^{+} T cells are known to facilitate CTL generation by licensing DCs to activate antigen-specific CD8^{+} T cells,[34] our studies failed to demonstrate a role for Piezo1 in affecting DC frequencies, activation or numbers in mice inoculated with OT2KO T cells (Figure S7b–g). Careful follow-up studies (Figure 6a,d–f) demonstrate that Piezo1 mediates the secretory profile of helper CD4^{+} T cells to optimize CD8^{+} T cell activation *in vitro*, with impaired CD25 and sustained PD-1 expression noted on activated, antigen-specific CD8^{+} T cells primed with both contact and contactless P1KO CD4 help.

In an LCMV infection model, Rafi Ahmed's group[43] previously reported that sustained CD25 expression on CD8^{+} T cells was associated with enhanced terminal effector differentiation. CD25^{hi}CD8^{+} T cells were shown to be more sensitive to IL-2 stimulation and demonstrated increased expression of effector genes (e.g., granzymes, IFNγ). In our own studies, we observe an increase in CD25 and IFNγ expression on CD8^{+} T cells up to 2 weeks after cryoablation of tumor-bearing WT mice (Figure 2f,g) that is absent in P1KO mice. Our *in vivo* ovalbumin vaccination model also demonstrates reduced frequencies of CD25^{+} and IFNγ^{+}Gzmb^{+} populations (Figure 5f,g,i) in responding OT1WT T cells exposed to P1KO OT2 T cell help. Additionally, no differences in activation or effector function were observed in CD8^{+} T cells lacking Piezo1 that were exposed to WT CD4^{+} T cell help (Figure 4). With this evidence, we believe that Piezo1 deletion induces an impaired CD4^{+} T cell secretory profile that leads to decreased frequencies of optimally activated CD25^{+}PD-1^{lo}-CD8^{+} T cells during the tumor immune response.

Preliminary signaling pathway analysis of mRNA profiling from *in vitro* activated P1KO versus WT CD4^{+} T cells consistently revealed genes involved in cytokine/cytokine receptor interaction pathways as being among the most enriched across a range of TCR stimulation strengths
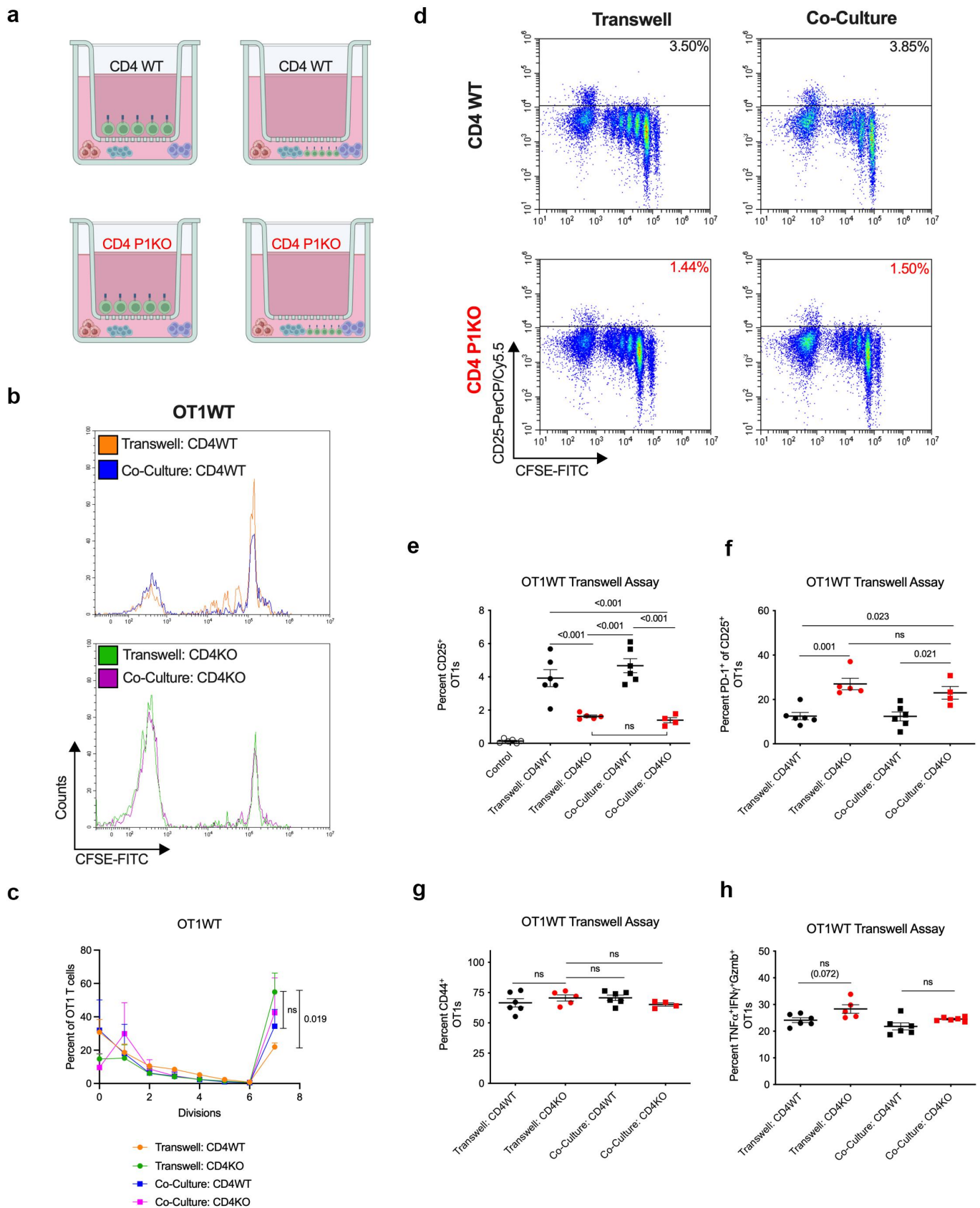
Figure 6. Antigen specific activation of CD8^{+} T cells in the presence of contact or contactless CD4 help. (a) Experimental strategy. Activated, polyclonal WT (top) or P1KO (bottom) CD4^{+} T cells were placed in transwell inserts above (left) or directly co-cultured with (right) naïve CD8^{+} OT1 T cells, RMS-OVA tumors, and irradiated splenocytes. (b) CFSE dilution curves for OT1 T cells cultured with WT (top) or P1KO (bottom) CD4^{+} T cells. (c) Quantification of cell divisions of OT1 T cells. (d) Flow analysis of OT1 T cells under various culturing conditions. Gating for CD25^{+} OT1s. (E) Percent CD25^{+} OT1 T cells. (f) Percent PD-1^{+} of CD25^{+} OT1s. (g) Percent TNFα^{+}/IFNγ^{+}/Gzmb^{+} OT1s undergoing at least 7 rounds of divisions. Plot of group means, standard error, and associated p-values between groups. ns = not statistically significant at an alpha of 0.05.

(*data not shown*). However, precise identification and validation of specific cytokine/cytokine receptor pair(s) as the primary contributor of the observed *in vitro* and *in vivo* phenomena warrant additional future studies.

In conclusion, we report a novel role for T cell Piezo1 in regulating tumor immune-mediated rejection. Tumor-bearing mice with Piezo1 deletion in the CD4$^+$ and CD8$^+$ T cell compartments have impaired rejection following immunostimulatory tumor cryoablation. Poor P1KO CD4$^+$ T cell helper responses underlie this phenomenon, resulting in a blunted activation of the CTL pool irrespective of the Piezo1 status of these CD8$^+$ T cells. Ultimately, Piezo1 mediates an optimal secretory profile for CD4$^+$ T cells, leading to the expansion of a cytotoxic CD25$^+$PD-1^{lo}CD8$^+$ T cell population during an inflammatory tumor challenge. Our results suggest that additional consideration is needed of CD4$^+$ T cell Piezo1 as a critical contributor in generating successful anti-tumor responses, especially in the development of immune modulating or adoptive T cell therapies. While it is not yet possible for pharmacologic targeting of T cell specific Piezo1 function for translational applications, our current study lays the foundation for such future efforts.

Acknowledgments

Disclosure statement

No potential conflict of interest was reported by the author(s).

Funding

ORCID

Melissa Bonner http://orcid.org/0000-0001-5043-1907
Jay T. Myers http://orcid.org/0000-0003-2574-0438
Byung-Gyu Kim http://orcid.org/0000-0002-8921-5061
Suzanne L. Tomchuck http://orcid.org/0000-0002-4068-3470
Alicia Santin http://orcid.org/0000-0002-5638-0861
Daniel Kingsley http://orcid.org/0000-0002-5767-6509
Sung Hee Choi http://orcid.org/0000-0002-8102-5538
Alex Y. Huang http://orcid.org/0000-0002-5701-4521

Author contributions

Conceptualization, m.a. and A.Y.H.; formal analysis, m.a. and A.Y.H.; resources, A.Y.H.; data curation, m.a., M.A., M.B., J.M., B.-G. K., S.L.T., A. S., D.K., S.-H. C.; writing – original draft preparation, m.a.; writing – review and editing, m.a., A.Y.H.; visualization, m.a., A.Y.H.; supervision, A.Y.H.; project administration, m.a., A.Y.H.; funding acquisition, m.a., A.Y.H. All authors have read and agreed to the published version of the manuscript.

Classification

Immunology and Inflammation

Data availability statement

The authors confirm that the data supporting the findings of this study are available within the article and its supplementary materials. The reagents are available from the corresponding author, A.Y.H., upon reasonable request and full execution of a Material Transfer Agreement agreed to by both parties.

References

1. Yao W, He J-C, Yang Y, Wang J-M, Qian Y-W, Yang T, Ji L. The prognostic value of tumor-infiltrating lymphocytes in hepatocellular carcinoma: a systematic review and meta-analysis. Sci Rep. 2017;7(1):7525. doi:10.1038/s41598-017-08128-1.

2. Gooden MJ, de Bock GH, Leffers N, Daemen T, Nijman HW. The prognostic influence of tumour-infiltrating lymphocytes in cancer: a systematic review with meta-analysis. Br J Cancer. 2011;105 (1):93–103. doi:10.1038/bjc.2011.189.

3. Orhan A, Vogelsang RP, Andersen MB, Madsen MT, Hölmich ER, Raskov H, Gögenur I. The prognostic value of tumour-infiltrating lymphocytes in pancreatic cancer: a systematic review and meta-analysis. Eur J Cancer. 2020;132:71–84. doi:10.1016/j.ejca.2020.03.013.

4. Piersiala K, Farrajota Neves da Silva P, Hjalmarsson E, Kolev A, Kågedal Å, Starkhammar M, Elliot A, Marklund L, Margolin G, Munck-Wikland E, et al. CD4 + and CD8 + T cells in sentinel nodes exhibit distinct pattern of PD-1, CD69, and HLA-DR expression compared to tumor tissue in oral squamous cell carcinoma. Cancer Sci. 2021;112(3):1048–1059. doi:10.1111/cas.14816.

5. Wang X, Liu Y. PD-L1 expression in tumor infiltrated lymphocytes predicts survival in triple-negative breast cancer. Pathol Res Pract. 2020;216(3):152802. doi:10.1016/j.prp.2019.152802.

6. Mita Y, Kimura MY, Hayashizaki K, Koyama-Nasu R, Ito T, Motohashi S, Okamoto Y, Nakayama T. Crucial role of CD69 in anti-tumor immunity through regulating the exhaustion of tumor-infiltrating T cells. Int Immunol. 2018;30(12):559–567. doi:10.1093/intimm/dxy050.

7. Zhang X, Kim T-H, Thauland TJ, Li H, Majedi FS, Ly C, Gu Z, Butte MJ, Rowat AC, Li S, et al. Unraveling the mechanobiology of immune cells. Curr Opin Biotechnol. 2020;66:236–245. doi:10.1016/j.copbio.2020.09.004.

8. Coste B, Mathur J, Schmidt M, Earley TJ, Ranade S, Petrus MJ, Dubin AE, Patapoutian A. Piezo1 and Piezo2 are essential components of distinct mechanically activated cation channels. Sci. 2010;330(6000):55–60. doi:10.1126/science.1193270.

9. Marshall KL, Saade D, Ghitani N, Coombs AM, Szczot M, Keller J, Ogata T, Daou I, Stowers LT, Bönnemann CG, et al. PIEZO2 in sensory neurons and urothelial cells coordinates urination. Nature. 2020;588(7837):290–295. doi:10.1038/s41586-020-2830-7.

10. Jairaman A, Othy S, Dynes JL, Yeromin AV, Zavala A, Greenberg ML, Nourse JL, Holt JR, Cahalan SM, Marangoni F, et al. Piezo1 channels restrain regulatory T cells but are dispensable for effector CD4 + T cell responses. Sci Adv. 2021;7(28). doi:10.1126/sciadv.abg5859.

11. Zhao Q, Zhou H, Chi S, Wang Y, Wang J, Geng J, Wu K, Liu W, Zhang T, Dong M-Q, et al. Structure and mechanogating mechanism

of the Piezo1 channel. Nature. 2018;554(7693):487–492. doi:10.1038/nature25743.

12. Aglialoro F, Hofsink N, Hofman M, Brandhorst N, van den Akker E. Inside out integrin activation mediated by PIEZO1 signaling in erythroblasts. Front Physiol. 2020;11:958. doi:10.3389/fphys.2020.00958.

13. Atcha H, Jairaman A, Holt JR, Meli VS, Nagalla RR, Veerasubramanian PK, Brumm KT, Lim HE, Othy S, Cahalan MD, et al. Mechanically activated ion channel Piezo1 modulates macrophage polarization and stiffness sensing. Nat Commun. 2021;12(1):3256. doi:10.1038/s41467-021-23482-5.

14. Wang Y, Yang H, Jia A, Wang Y, Yang Q, Dong Y, Hou Y, Cao Y, Dong L, Bi Y, et al. Dendritic cell Piezo1 directs the differentiation of T(H)1 and T(reg) cells in cancer. Elife. 2022;11:11. doi:10.7554/eLife.79957.

15. Liu CSC, Raychaudhuri D, Paul B, Chakrabarty Y, Ghosh AR, Rahaman O, Talukdar A, Ganguly D. Cutting Edge: Piezo1 Mechanosensors Optimize Human T Cell Activation. J Immunol. 2018;200(4):1255–1260. doi:10.4049/jimmunol.1701118.

16. Alshebremi M, Tomchuck SL, Myers JT, Kingsley DT, Eid S, Abiff M, Bonner M, Saab ST, Choi SH, Huang AYC, et al. Functional tumor cell-intrinsic STING, not host STING, drives local and systemic antitumor immunity and therapy efficacy following cryoablation. J Immunother Cancer. 2023;11(8):e006608. doi:10.1136/jitc-2022-006608.

17. Meadors JL, Cui Y, Chen Q-R, Song YK, Khan J, Merlino G, Tsokos M, Orentas RJ, Mackall CL. Murine rhabdomyosarcoma is immunogenic and responsive to T-cell-based immunotherapy. Pediatr Blood Cancer. 2011;57(6):921–929. doi:10.1002/pbc.23048.

18. Weigel BJ, Rodeberg DA, Krieg AM, Blazar BR. CpG oligodeoxynucleotides potentiate the antitumor effects of chemotherapy or tumor resection in an orthotopic murine model of rhabdomyosarcoma. Clin Cancer Res. 2003;9:3105–3114.

19. Dorand RD, Nthale J, Myers JT, Barkauskas DS, Avril S, Chirieleison SM, Pareek TK, Abbott DW, Stearns DS, Letterio JJ, et al. Cdk5 disruption attenuates tumor PD-L1 expression and promotes antitumor immunity. Sci. 2016;353(6297):399–403. doi:10.1126/science.aae0477.

20. Uhlen M, Oksvold P, Fagerberg L, Lundberg E, Jonasson K, Forsberg M, Zwahlen M, Kampf C, Wester K, Hober S, et al. Towards a knowledge-based human protein atlas. Nat Biotechnol. 2010;28(12):1248–1250. doi:10.1038/nbt1210-1248.

21. Ranade SS, Qiu Z, Woo S-H, Hur SS, Murthy SE, Cahalan SM, Xu J, Mathur J, Bandell M, Coste B, et al. Piezo1, a mechanically activated ion channel, is required for vascular development in mice. Proc Natl Acad Sci U S A. 2014;111(28):10347–10352. doi:10.1073/pnas.1409233111.

22. Jiang X, Wang J, Deng X, Xiong F, Ge J, Xiang B, Wu X, Ma J, Zhou M, Li X, et al. Role of the tumor microenvironment in PD-L1/PD-1-mediated tumor immune escape. Mol Cancer. 2019;18(1):10. doi:10.1186/s12943-018-0928-4.

23. Oh DY, Fong L. Cytotoxic CD4(+) T cells in cancer: expanding the immune effector toolbox. Immunity. 2021;54(12):2701–2711. doi:10.1016/j.immuni.2021.11.015.

24. Quezada SA, Simpson TR, Peggs KS, Merghoub T, Vider J, Fan X, Blasberg R, Yagita H, Muranski P, Antony PA, et al. Tumor-reactive CD4(+) T cells develop cytotoxic activity and eradicate large established melanoma after transfer into lymphopenic hosts. J Exp Med. 2010;207(3):637–650. doi:10.1084/jem.20091918.

25. Miwa S, Yamamoto N, Hayashi K, Takeuchi A, Igarashi K, Tsuchiya H. Recent advances and challenges in the treatment of rhabdomyosarcoma. Cancers Basel. 2020;12(7):12(7. doi:10.3390/cancers12071758.

26. Jardine L, Barge D, Ames-Draycott A, Pagan S, Cookson S, Spickett G, Haniffa M, Collin M, Bigley V. Rapid detection of dendritic cell and monocyte disorders using CD4 as a lineage marker of the human peripheral blood antigen-presenting cell compartment. Front Immunol. 2013;4:495. doi:10.3389/fimmu.2013.00495.

27. Vremec D, Pooley J, Hochrein H, Wu L, Shortman K. CD4 and CD8 expression by dendritic cell subtypes in mouse thymus and spleen. J Immunol. 2000;164(6):2978–2986. doi:10.4049/jimmunol.164.6.2978.

28. Ferris ST, Durai V, Wu R, Theisen DJ, Ward JP, Bern MD, Davidson JT, Bagadia P, Liu T, Briseño CG, et al. cDC1 prime and are licensed by CD4(+) T cells to induce anti-tumour immunity. Nature. 2020;584(7822):624–629. doi:10.1038/s41586-020-2611-3.

29. Askew D, Harding CV. Antigen processing and CD24 expression determine antigen presentation by splenic CD4+ and CD8+ dendritic cells. Immunology. 2008;123(3):447–455. doi:10.1111/j.1365-2567.2007.02711.x.

30. den Haan JM, Lehar SM, Bevan MJ. CD8(+) but not CD8(-) dendritic cells cross-prime cytotoxic T cells in vivo. J Exp Med. 2000;192(12):1685–1696. doi:10.1084/jem.192.12.1685.

31. Ahrends T, Spanjaard A, Pilzecker B, Bąbała N, Bovens A, Xiao Y, Jacobs H, Borst J. CD4(+) T cell help confers a cytotoxic T cell effector program including coinhibitory receptor downregulation and increased tissue invasiveness. Immunity. 2017;47(5):848–861. e5. doi:10.1016/j.immuni.2017.10.009.

32. Bedoui S, Heath WR, Mueller SN. CD4(+) T-cell help amplifies innate signals for primary CD8(+) T-cell immunity. Immunol Rev. 2016;272(1):52–64. doi:10.1111/imr.12426.

33. Zhang S, Zhang H, Zhao J. The role of CD4 T cell help for CD8 CTL activation. Biochem Biophys Res Commun. 2009;384(4):405–408. doi:10.1016/j.bbrc.2009.04.134.

34. Smith CM, Wilson NS, Waithman J, Villadangos JA, Carbone FR, Heath WR, Belz GT. Cognate CD4(+) T cell licensing of dendritic cells in CD8(+) T cell immunity. Nat Immunol. 2004;5(11):1143–1148. doi:10.1038/ni1129.

35. Cella M, Scheidegger D, Palmer-Lehmann K, Lane P, Lanzavecchia A, Alber G. Ligation of CD40 on dendritic cells triggers production of high levels of interleukin-12 and enhances T cell stimulatory capacity: T-T help via APC activation. J Exp Med. 1996;184(2):747–752. doi:10.1084/jem.184.2.747.

36. Caux C, Massacrier C, Vanbervliet B, Dubois B, Van Kooten C, Durand I, Banchereau J. Activation of human dendritic cells through CD40 cross-linking. J Exp Med. 1994;180(4):1263–1272. doi:10.1084/jem.180.4.1263.

37. Borst J, Ahrends T, Bąbała N, Melief CJM, Kastenmüller W. CD4(+) T cell help in cancer immunology and immunotherapy. Nat Rev Immunol. 2018;18(10):635–647. doi:10.1038/s41577-018-0044-0.

38. Shah W, Yan X, Jing L, Zhou Y, Chen H, Wang Y. A reversed CD4/CD8 ratio of tumor-infiltrating lymphocytes and a high percentage of CD4(+)FOXP3(+) regulatory T cells are significantly associated with clinical outcome in squamous cell carcinoma of the cervix. Cell Mol Immunol. 2011;8(1):59–66. doi:10.1038/cmi.2010.56.

39. Wang K, Shen T, Siegal GP, Wei S. The CD4/CD8 ratio of tumor-infiltrating lymphocytes at the tumor-host interface has prognostic value in triple-negative breast cancer. Hum Pathol. 2017;69:110–117. doi:10.1016/j.humpath.2017.09.012.

40. Castilho JL, Bian A, Jenkins CA, Shepherd BE, Sigel K, Gill MJ, Kitahata MM, Silverberg MJ, Mayor AM, Coburn SB, et al. CD4/CD8 ratio and Cancer risk among adults with HIV. J Natl Cancer Inst. 2022;114(6):854–862. doi:10.1093/jnci/djac053.

41. Serrano-Villar S, Sainz T, Lee SA, Hunt PW, Sinclair E, Shacklett BL, Ferre AL, Hayes TL, Somsouk M, Hsue PY, et al. HIV-infected individuals with low CD4/CD8 ratio despite effective antiretroviral therapy exhibit altered T cell subsets, heightened CD8+ T cell activation, and increased risk of non-AIDS morbidity and mortality. PLoS Pathog. 2014;10(5):e1004078. doi:10.1371/journal.ppat.1004078.

42. Lu W, Mehraj V, Vyboh K, Cao W, Li T, Routy J-P. CD4: CD8 ratio as a frontier marker for clinical outcome, immune dysfunction and viral reservoir size in virologically suppressed HIV-positive patients. J Int AIDS Soc. 2015;18(1):20052. doi:10.7448/IAS.18.1.20052.

43. Kalia V, Sarkar S, Subramaniam S, Haining WN, Smith KA, Ahmed R. Prolonged interleukin-2Rα expression on virus-specific CD8+ T cells favors terminal-effector differentiation in vivo. Immunity. 2010;32(1):91–103. doi:10.1016/j.immuni.2009.11.010.